Supporting information

Orally pH-activated "nano-bomb" carrier combined with berberine by regulating gene silencing and gut microbiota for site-specific treatment of ulcerative colitis

Mei Yang[1,2], Chunhua Yang[3], Yujie Zhang[1,2], Xiangji Yan[1,2], Yana Ma[1,2], Yuanyuan Zhang[1,2], Yameng Cao[1,2], Qiuran Xu[4,5*], Kangsheng Tu[6*] and Mingzhen Zhang[1,2*]

Affiliations:

1. School of Basic Medical Sciences, Xi'an Key Laboratory of Immune Related Diseases, Xi'an Jiaotong University, Xi'an, Shaanxi, 710061, China
2. Key Laboratory of Environment and Genes Related to Diseases, Xi'an Jiaotong University, Ministry of Education, Xi'an, Shaanxi, 710061, China
3. Institute for Biomedical Sciences, Center for Diagnostics and Therapeutics, Digestive Disease Research Group, Georgia State University, Atlanta, Georgia, 30302, United States.
4. Laboratory of Tumor Molecular Diagnosis and Individualized Medicine of Zhejiang Province, Zhejiang Provincial People's Hospital, Affiliated People's Hospital, Hangzhou Medical College, Hangzhou, Zhejiang, 310014, China
5. Research Center of Diagnosis and Treatment Technology for Hepatocellular Carcinoma of Zhejiang Province, Hangzhou, Zhejiang, 310009, China
6. Department of Hepatobiliary Surgery, the First Affiliated Hospital of Xi'an Jiaotong University, Xi'an, Shaanxi, 710061, China

*Authors for correspondence
Qiuran Xu (ORCID: 0000-0003-2171-9279)
Email address: windway626@sina.com

Kangsheng Tu (ORCID: 0000-0002-0032-1459)
Email address: tks0912@foxmail.com

Mingzhen Zhang (ORCID: 0000-0002-4686-6526)
Email address: mzhang21@xjtu.edu.cn

Materials and methods

Materials

PLGA (lactide:glycolide, 75:25; MW=4-15 kDa), poly (vinyl alcohol) (PVA, 87-90% hydrolyzed, MW=30-70 kDa) and berberine chloride were purchased from Sigma. PLGA-PEG-Mal (PLGA MW=10,000 & PEG MW=2,000) were obtained from Nanosoft Biotechnology (Winston-Salem, NC, America). Sulfhydryl-modified hyaluronic acid was purchased from Xi'an Ruixi Biological Technology Co. (Shaanxi, China). Agarose, ethidium bromide and loading buffer were purchased from Generay Biotechnology. DPPC was purchased from Avanti. Chitosan oligosaccharide of pharmaceutical grade (MW=1.5 kDa, 95% deacetylation) was purchased from Qingdao BZ Oligo Biotech Co., and methyl aminomethanimidothioate hydroiodide was purchased from J&K Scientific Ltd. (Beijing, China). Fluorescent lipophilic dyes (DiL and DiR) were purchased from Promokine (Heidelberg, Germany).

Characterization of NPs

Dynamic light scattering (DLS) and Transmission Electron Microscope (TEM) were used to characterize the NPs. The size and zeta potential of NPs were determined using a Malvern Zetasizer Apparatus (Worcestershire, UK) at room temperature. NPs were first incubated with phosphate buffer solution (pH 7.4 and 6.0) or sodium acetate buffer solution (pH 5.0) for 6 h, then stained with uranyl acetate (2%, w/v) before TEM (JEOL JEM-2100, Japan) observation. To calculate encapsulation efficiency and loading content of siCD98 in NPs, FAM-siCD98 was loaded into the NPs. NPs (5mg) were dissolved in 1ml of dichloromethane and extracted using DEPC water. The fluorescence of FAM at 518nm was measured by a fluorescence spectrometer (HITACHI, F-4700, Japan) to determine siCD98 in NPs. The encapsulation efficiency of the siCD98 was calculated as the ratio of the amount of siCD98 encapsulated in the NPs to the total amount of siCD98 for encapsulation. The loading content of the siCD98 in the NPs was calculated

as the ratio of the amount of siCD98 encapsulated in the NPs to the total amount of NPs, including the siRNA.

Real-time PCR

Total RNA was extracted from activated Raw 264.7 cells using an RNAeasy ™ Animal RNA Extraction Kit (Beyotime, Shanghai, China) according to the manufacturer's instructions. The yield and quality of extracted RNA were verified with the nanodrop (DS-11 FX +, DeNovix, America). cDNA was generated from the total RNA isolated above using the BeyoRT ™ III cDNA Synthesis Premix (5X) with GDNA EZeraser (Beyotime, Shanghai, China). Expression of target mRNAs was quantified by real-time reverse transcription-polymerase chain reaction (qRT-PCR) (CFX96™Real time system, Bio-Rad, America) using Roche SYBR Green qPCR Master Mix. The primers used in this experiment are shown in **Table S1**. RNA extraction from colon tissues and qRT-PCR follow the same steps as above.

***In vitro* nanoparticles stability testing**

Simulated intestinal fluid consisted of 3 mM sodium taurocholate, 0.2 mM lecithin, 19.12 mM maleic acid, 34.8 mM sodium hydroxide, 68.62 mM sodium chloride, and 1 mg/mL pancreatin. 50 mL of intestinal fluid was incubated with 4 mg of HA-siCD98@NPs at 37 °C. The size and PDI index of NPs were measured at a fixed time every day for 7 consecutive days.

Histological analyses of tissue sections by H&E staining

The colon tissues, parts of the GI tract, and different organs of the mice were fixed with tissue fixative for 72 h, and then dehydrated for paraffin embedding. Tissues were sectioned at 6 μm thickness and stained with H&E using standard protocols. Images were acquired using a microscope. Histological scores were assigned by experimenters "blinded" to sample identity. Colonic epithelial damage was assigned scores as follows: 0 = normal; 1 = hyperproliferation, irregular crypts, and goblet cell loss; 2 = mild to moderate

crypt loss (10–50%); 3 = severe crypt loss (50–90%); 4 = complete crypt loss, surface epithelium intact; 5 = small-to-medium-sized ulcer (<10 crypt widths); 6 = large ulcer (≥ 10 crypt widths). Infiltration with inflammatory cells was assigned scores separately for mucosa (0=normal, 1=mild, 2=modest, 3=severe), submucosa (0=normal, 1=mild to modest, 2=severe), and muscle/serosa (0=normal, 1=moderate to severe). Scores for colonic epithelial damage and inflammatory cell infiltration were added up, resulting in a total scoring range of 0-12.

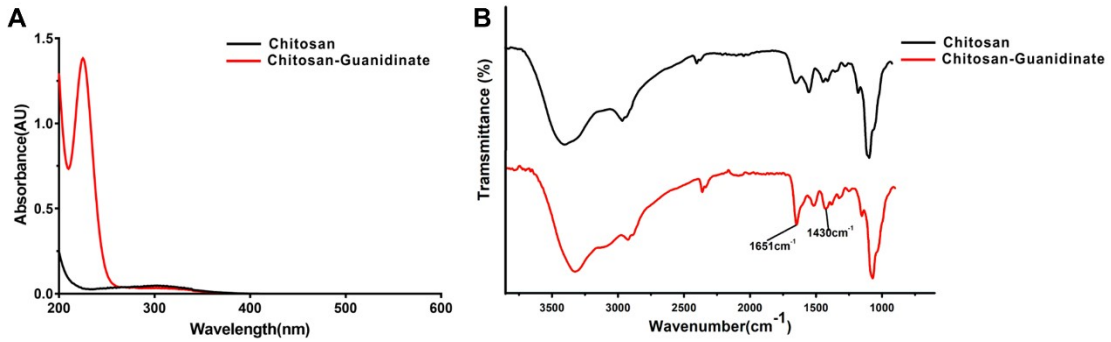

Fig. S1 Characterization of the modification of chitosan with guanidine. **A.** UV-Vis absorbance of chitosan before and after modification with guanidine. The specific absorption peak at 225nm of guanidine in chitosan-guanidine indicates the successful modification of guanidine onto chitosan. **B.** FT-IR spectra of chitosan and chitosan-guanidinate showing the absorption of guanidine group at 1430 cm^{-1} and 1651 cm^{-1}, in which 1430 cm^{-1} is the saturated C-H deformation vibration absorption peak and 1650 cm^{-1} is the absorption peak of C=N stretching vibration in guanidine group. UV-Vis: Ultraviolet-visible light, and FT-IR: Fourier transform infrared spectroscopy.

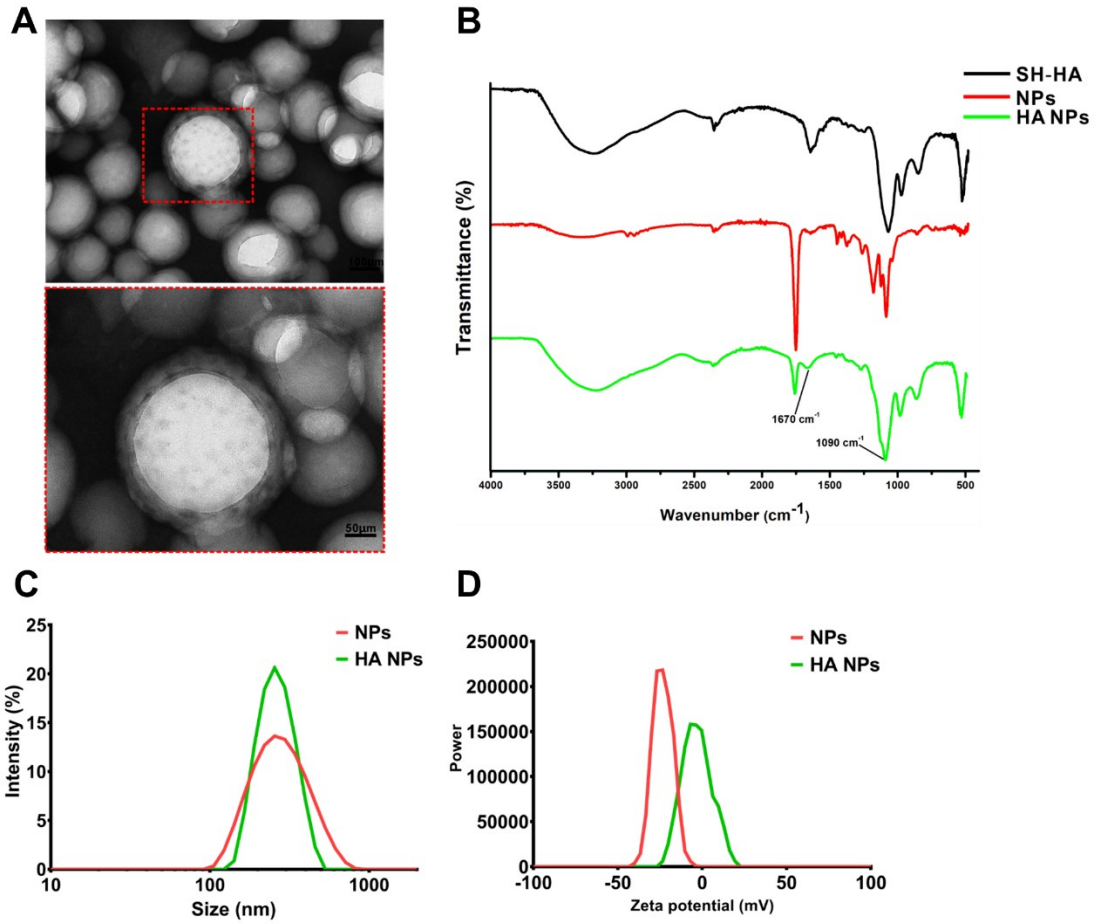

Fig. S2 Characterizations of nanoparticles modified with hyaluronic acid (HA). **A.** TEM images of CG-CO_2@NPs modified with HA. **B.** FT-IR spectra of HA-CG-CO_2@NPs (HA NPs) showing the different absorption at 1670 cm^{-1}, and 1090 cm^{-1}, in which 1670 cm^{-1} is the saturated C=C deformation vibration absorption peak, 1090 cm^{-1} is the absorption peak of C-S stretching vibration in the Michael addition reaction of maleimide and thiol. **C-D.** Size distribution and zeta potential of CG-CO_2@NPs and HA-CG-CO_2@NPs were determined by dynamic light scattering (DLS). FT-IR: Fourier transform infrared spectroscopy.

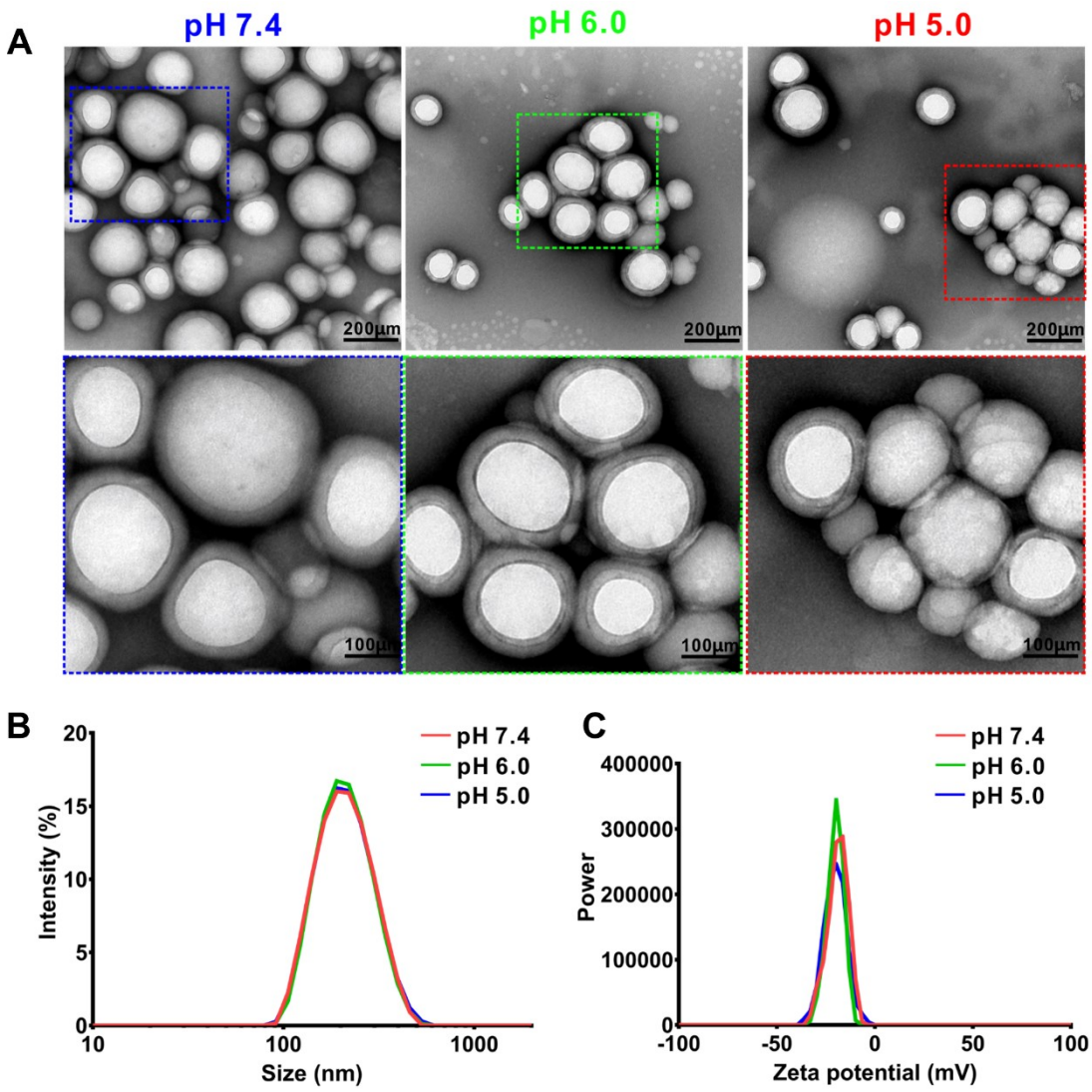

Fig. S3 Nanoparticles synthesized using chitosan-guanidinate without CO_2 (CG@NPs) were not qualified with pH-activated "nanobomb effect". **A.** TEM images of the nanoparticles under different pH conditions showing that the nanoparticles could maintain their intact spherical morphology and core-shell structure and were not responsive to low pH treatments (pH 6.0 and pH 5.0). **B-C.** The size distribution and zeta potential of nanoparticles under different pH were determined by dynamic light scattering (DLS).

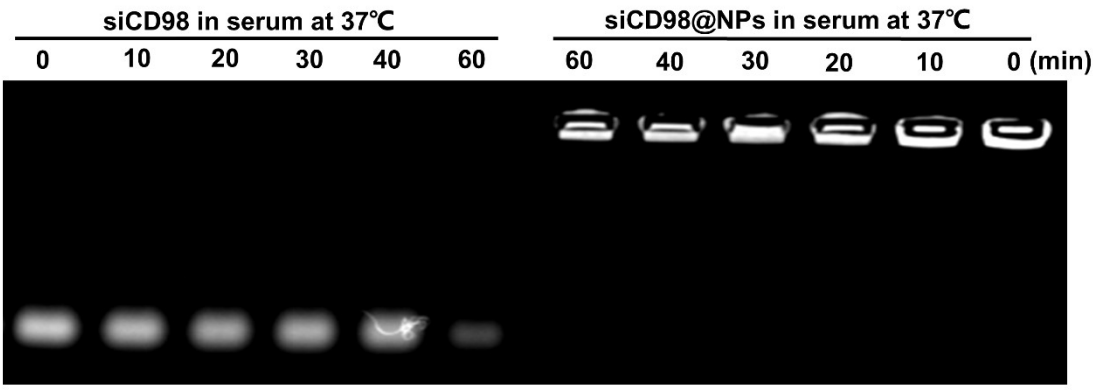

Fig. S4 The stability of free siCD98 compared to siCD98 encapsulated in the nanoparticles (siCD98@NPs) was evaluated by electrophoretic gel assay after incubating them in serum at 37 °C for up to 60 min.

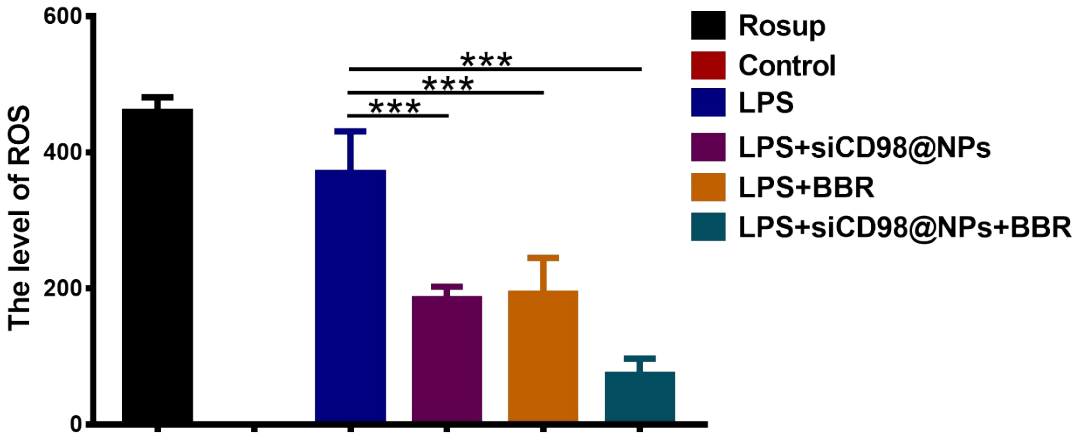

Fig. S5 ROS levels with different treatments were evaluated, n=6.

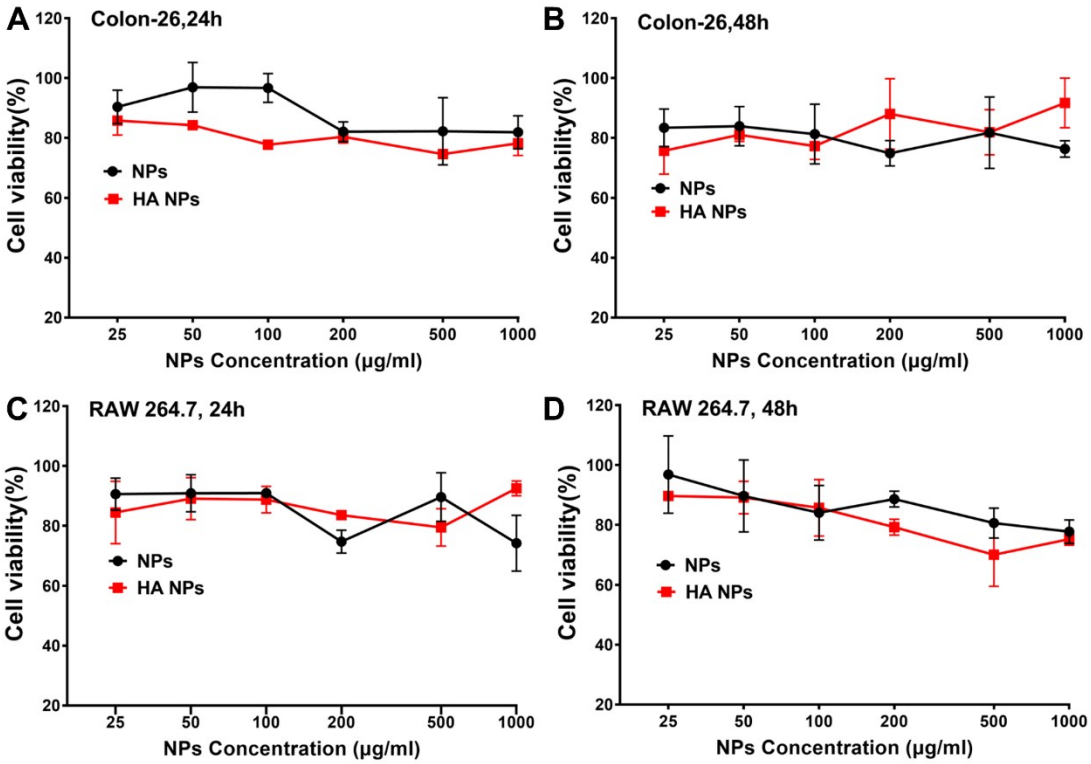

Fig. S6 The biocompatibility of CG-CO_2@NPs (NPs) and HA-CG-CO_2@NPs (HA NPs) *in vitro* were evaluated. Colon-26 cells and RAW 264.7 cells were incubated with nanoparticles with different concentrations for 24 h and 48 h, respectively, then, the cell viabilities were assessed by MTT assay, n=6.

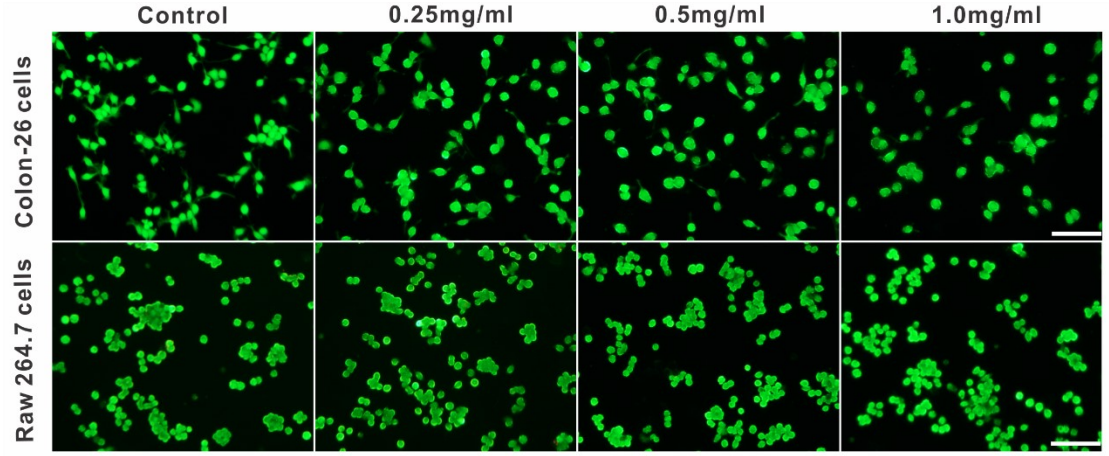

Fig. S7 Cell viabilities were evaluated by Calcein-AM/PI (propidium iodide) staining. Colon-26 cells and RAW 264.7 cells were incubated with nanoparticles with different concentrations for 24 h, then, the cell viabilities were assessed by Calcein-AM/PI staining. Scale bar: 100 μm.

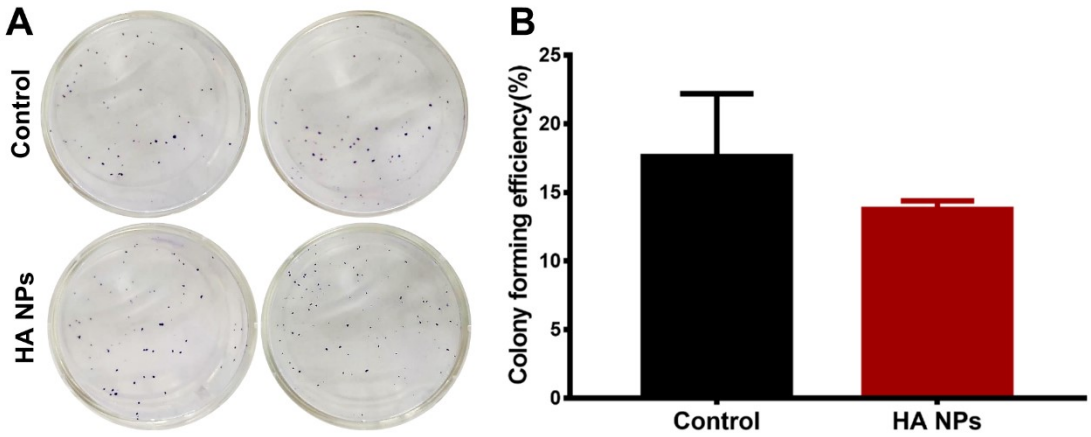

Fig. S8 Colony formation assay was used to evaluate the cell proliferation after treated with HA-CG-CO_2@NPs (HA NPs), n=6.

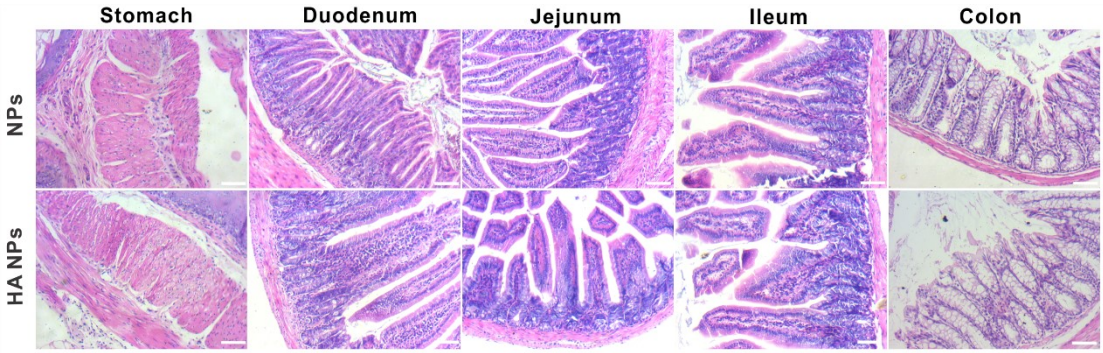

Fig. S9 Tissues from different parts of gastrointestinal (GI) tracts were stained by H&E after orally administration of CG-CO_2@NPs (NPs) and HA-CG-CO_2@NPs (HA NPs) for 7 days, n=3. Scale bar: 100 μm.

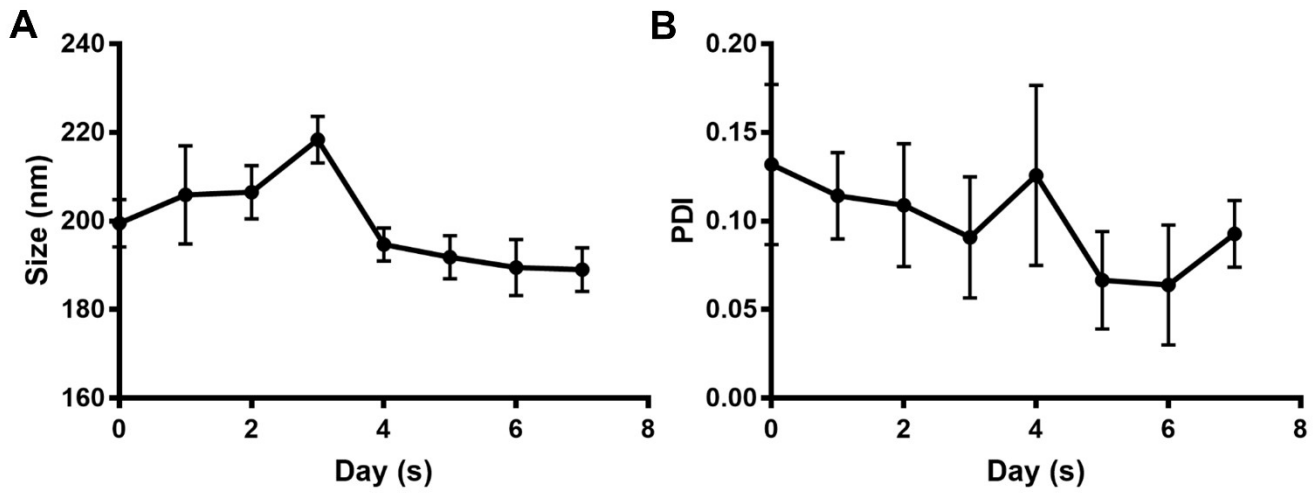

Fig. S10 The size (A) and polymer dispersity (PDI) index (B) of the nanoparticles in the simulated intestinal fluid over 7 consecutive days of measurements.

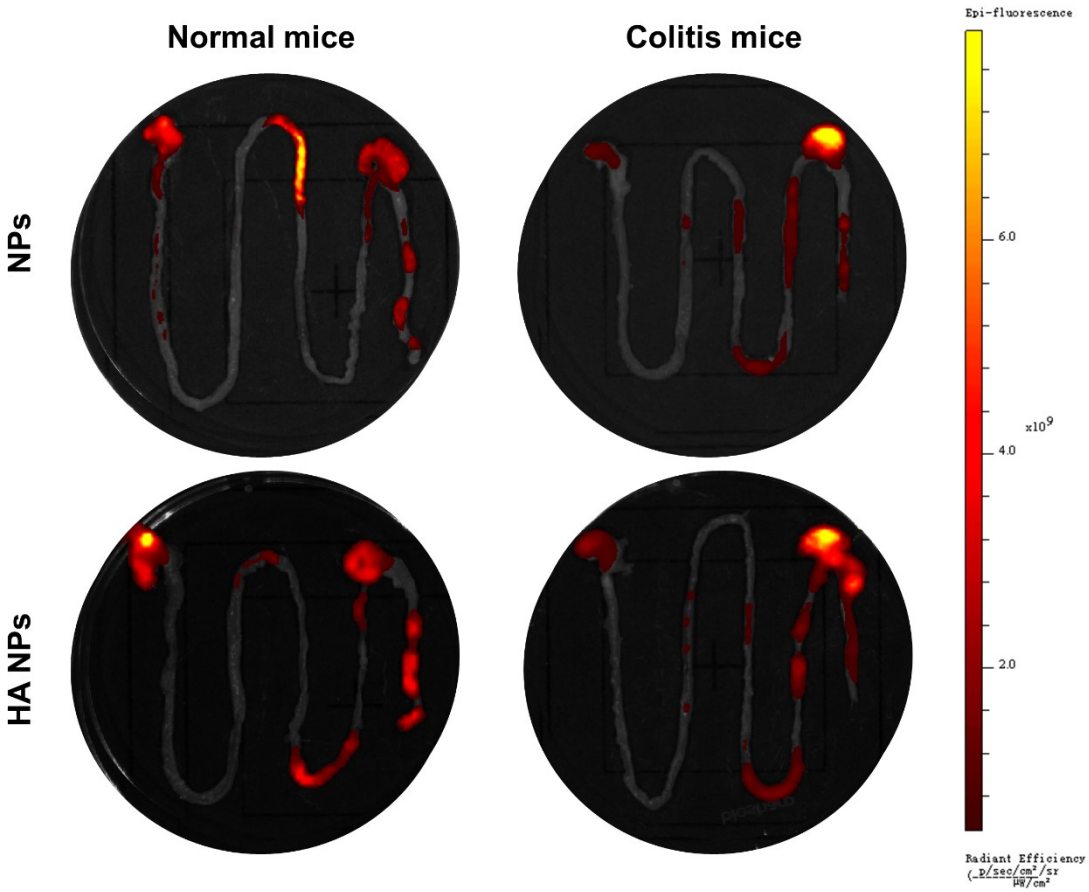

Fig. S11 DiR-labeled CG-CO_2@NPs (NPs) and HA-CG-CO_2@NPs (HA NPs) in hydrogel were orally administrated to normal and colitis mice. Images were obtained at 12 h post-administration using an *in vivo* imaging system (IVIS).

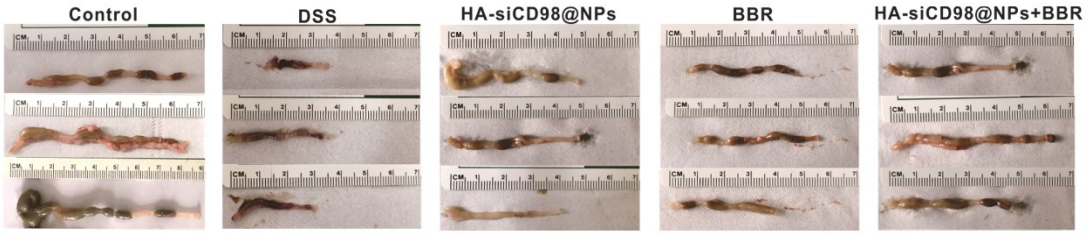

Fig. S12 The length of colons from different treatment mice was measured on day 8 after euthanasia.

Table S1. Primers used for real-time PCR.

Gene name	Forward primer (5'-3')	Reverse primer (5'-3')
CD98	GAGGACAGGCTTTTGATTGC	TCCAGGCTTTGGGCATCA
TNF-alpha	AGGCTGCCCCGACTACGT	GACTTTCTCCTGGTATGAGATAGCAAA
IL-6	AGGCTGCCCCGACTACGT	TTGCCATTGCACAACTCTTTTC
IL-1beta	TCGCTCAGGGTCACAAGAAA	CATCAGAGGCAAGGAGGA AAA C
36B4	TCCAGGCTTTGGGCATCA	CTTTATCAGCTGCACATCACTCAGA